AIAA 81-4156

Three-Dimensional Oscillatory Piecewise Continuous-Kernel Function Method—Part I: Basic Problems

I. Lottati* and E. Nissim†
Technion—Israel Institute of Technoloy, Haifa, Israel

The two-dimensional subsonic, piecewise continuous-kernel function method used for studying either oscillatory or steady flows is extended in the present work to three-dimensional problems involving finite-span wings. The work treats questions associated with the choice of spanwise pressure polynomials, spanwise collocation points, and numerical integration techniques that need be faced by this method. A subsequent paper contains results which confirm the accuracy of the method, its rapid convergence, and its very high efficiency in terms of computational time. The method is tested for a limited class of geometrical discontinuities (i.e., at the wing root only). A third paper contains additional results which relate to a wider class of problems associated with geometrical discontinuities.

Introduction

GEOMETRICAL discontinuities have become common in modern airplane wings, including not only control surface deflections but also wing chord discontinuities such as those existing at the root of a delta wing (discontinuity in the first derivative of the chord *along* the span), at leading-edge extensions, or at wing surface break points. Since these geometrical discontinuities lead to pressure singularities at the same geometrical locations, it is necessary to know the exact form of these pressure singularities if the use of the kernel function method (KFM) is contemplated. The lattice methods (i.e., the vortex or doublet) can successfully cope with unknown pressure singularities if their location is known, but they require a relatively large number of unknowns ("boxes") for convergence which at times leads to a relatively large residual error at the converged values.[1,2] In Refs. 1 and 2, a different method is proposed which represents the pressure distribution by a set of piecewise continuous polynomials spanning the regions between adjoining singularities (also referred to as "boxes") and employs the KFM for solution of the pressure coefficients. It is shown in Refs. 1 and 2 where this two-dimensional problem was treated that such an approach, referred to as the piecewise continuous-kernel function method (PCKFM), has the ability to treat pressure discontinuities in a manner similar to the doublet-lattice method, with the added accuracy and rapid convergence characteristics of the kernel function method. In addition, it is not essential to determine the nature or form of the pressure singularities that might exist along some of the boundaries forming each box. However, to accelerate convergence, pressure singularities are assumed to be known only along the boundaries of the wing; or more specifically, the form of the leading-edge (LE), trailing-edge (TE), and wing-tip pressure singularities are assumed to be known and are treated in the analysis. All other pressure singularities are ignored during the analysis and their consideration is limited to the determination of the boundaries for the different boxes.

The basic problems associated with the two-dimensional PCKFM were treated in Refs. 1 and 2. These problems included the determination of orthogonal pressure polynomials for boxes with different known pressure singularities along their boundaries, the determination of the collocation points associated with the assumed pressure polynomials, the determination of the desired number of boxes, and the number of orthogonal polynomials required in each box. These problems will be addressed again while attempting to extend the PCKFM to wings with finite spans. Additional problems arising in three-dimensional flow configurations involve the formulation of numerical techniques which are required for the successful application of the method. These techniques, which are useful beyond the methods described in this work, will be developed herein.

Wing-Tip Pressure Singularity and Associated Collocation Points

As already stated, the pressure singularities are assumed to be known only along the boundaries of the wing. The nature of the LE and TE singularities and other associated chordwise orthogonal pressure polynomials and chordwise collocation points were treated in Refs. 1 and 2 in connection with the two-dimensional case. The nature of the wing-tip pressure singularity needs a brief discussion. Assume for example that a geometrical discontinuity, such as a break point, exists on the wing to be treated (see Fig. 1). Each wing has to be represented by at least two boxes, one at the tip region and the other at the root region. It seems clear that the choice of the normal wing-tip singularity (of the form $\sqrt{1-\eta^2}$) for the outboard box is not justified since it includes the singularities of both wing tips, whereas the outboard box is exposed to a single singularity only. This latter singularity assumes the form of $\sqrt{1-\eta}$ for the right wing and the form of $\sqrt{1+\eta}$ for the left wing. In the following, reference to the right wing only will be made in connection with the wing-tip singularity which will be assumed to be of the form $\sqrt{1-\eta}$. The spanwise polynomials which are orthogonal to the above wing-tip singularity are identical in form to the polynomials associated with the TE box in the two-dimensional case treated in Refs. 1 and 2 (where the singularity at the TE is given by $\sqrt{1-x}$).

The pressure distribution in each of the boxes formed by the PCKFM can therefore be represented in general terms by the following expression.

$$\Delta p(\zeta,\eta)/q = \sum_{j=1}^{ns}\sum_{i=1}^{nc} A_m W(\eta) p_j(\eta) w(\zeta) p_i(\zeta) \qquad (1)$$

where Δp represents the pressure distribution in the box, q the dynamic pressure, A_m a scalar coefficient, ns the number of spanwise polynomials, nc the number of chordwise polynomials, and m is given by

$$m = (j-1)nc + i$$

Received Jan. 7, 1980; revision received Dec. 22, 1980.

*Lecturer, Department of Aeronautical Engineering.
†Professor, Department of Aeronautical Engineering. Member AIAA.

The parameters ζ and η represent the coordinates in the chordwise and spanwise directions, respectively. $W(\eta)$ and $w(\zeta)$ represent the assumed singularities in the spanwise and chordwise directions, respectively. If no singularities exist in either one or both directions $W(\eta)$ or $w(\zeta)$ or both are assumed to be equal to 1. $w(\zeta)$ is shown[1,2] to be given by the following expressions:

$$w(\zeta) = \frac{1}{\sqrt{1+\zeta}} \quad \text{for a LE box}$$

$$= \sqrt{1-\zeta} \quad \text{for a TE box}$$

$$= 1 \quad \text{for an intermediate box}$$

$$= \sqrt{\frac{1-\zeta}{1+\zeta}} \quad \text{for a box which includes both an LE and a TE along its boundaries}$$

and $p_i(\zeta)$ is a polynomial of degree $(i-1)$ which is orthogonal to the singularity represented by $w(\zeta)$ (for more details see Refs. 1 and 2). $W(\eta)$ can assume either the value of 1 (for any box which does not have the wing tip along its boundary) or the value of $\sqrt{1-\eta}$. The pressure polynomial $P_j(\eta)$ is therefore a polynomial of degree $(j-1)$ which is orthogonal to the singularity represented by $W(\eta)$. Hence, for example when $W(\eta)=1$, $P_j(\eta)$ represents the Legendre polynomial.

An attempt will now be made to determine the spanwise downwash collocation points resulting from the use of the aforementioned pressure polynomials (the chordwise locations are assumed to be the same as in the two-dimensional case). These collocation points will clearly be applicable to the wing-tip box only. The method adopted for this purpose follows the lines proposed by Hsu,[3] which were successfully applied in the two-dimensional case.[1,2] It can be shown[3] that the overall downwash error is minimized if the collocation points in each box are located at the zeros of the downwash polynomial obtained from the pressure polynomial of one order higher than the highest polynomial used in the box (see also Appendix). These zeros are determined numerically by evaluating the downwash over a large number of spanwise points resulting from orthogonal polynomials of increasing order. The results obtained indicate that the zeros of the downwash polynomials coincide with the zeros of the pressure polynomials. In other words, the collocation points should be located at the zeros of the polynomials which are orthogonal to the wing tip singularity $\sqrt{1-\eta}$ (see Appendix).

Figure 2 shows a comparison between the collocation points obtained by the method just described (the illustration relates to two spanwise collocation points) and those proposed by Multhopp. It can be seen that the new collocation points are substantially inboard of the Multhopp points and that therefore their incorporation into the numerical solution of the wing problem is essential. This point will further be elaborated in a later section. The variation of these collocation points with Mach number M and reduced frequency k was found to be small. Therefore, the aforementioned collocation points are applicable for all cases of subsonic unsteady flow problems.

Numerical Problems Associated with the PCKFM

The use of kernel function methods require the integration over the wing of expressions which include the kernel function. In the two-dimensional case,[1,2] these integrations were performed analytically. In the three-dimensional case however, it is found impossible to extend the analytical methods of integration employed in the two-dimensional case and therefore resort is made to numerical integration techniques. Application of the integration techniques normally used in wing theory gives rise to difficulties associated with the nature of the strong singularity of the kernel function (second-order pole). These difficulties are explained in the following sections.

Spanwise Integration of the Kernel-Downwash Expression

The relationship between the pressure distribution over the wing and its resulting downwash is given by

$$w(x,y) = \frac{1}{8\pi} \int_S \int \frac{\Delta P(\zeta,\eta)}{q} \frac{K_p(x-\zeta,y-\eta,k,M)}{(y-\eta)^2} \, d\zeta d\eta \qquad (2)$$

where

$w(x,y)$ = vertical velocity (downwash at any collocation point (x,y) of the wing
$K_p(x-\zeta,y-\eta,k,M)$ = modified kernel function (without the second pole singularity)
k = reduced frequency
M = Mach number
S = area of wing surface

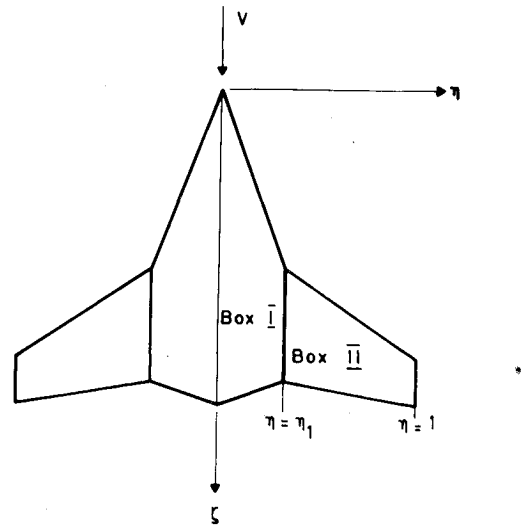

Fig. 1 Example of wing with geometrical discontinuities (break points in both LE and TE).

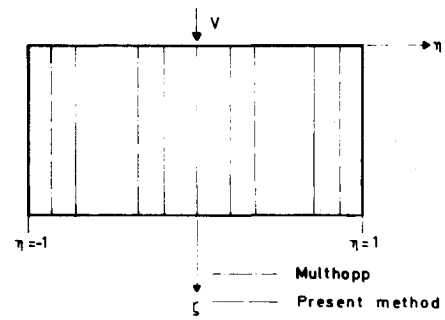

Fig. 2 Comparison between collocation points obtained by present method and those proposed by Multhopp.

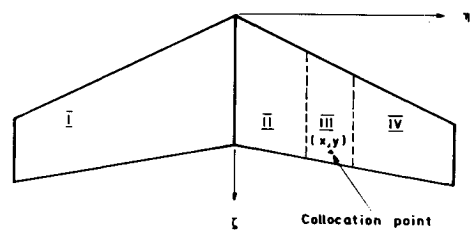

Fig. 3 Wing division into regions to accomplish spanwise integration.

Table 1 Influence of varying the spanwise width of singular region III on the convergence of the aerodynamic coefficients (delta wing ($\mathcal{R}=2$) in a steady incompressible flow)[a]

Width of region III	C_{L_α}	C_{M_α}	CPU, s
0.30	− 2.387	− 2.888	6.54
0.20	− 2.701	− 3.375	6.83
0.10	− 4.877	− 6.470	7.33
0.06	−42.464	−57.864	7.38
0.02	− 0.380	− 0.438	7.56

[a] See footnotes 1-5, 7.‡

Table 2 Influence of varying the spanwise width of singular region III on the convergence of the aerodynamic coefficients (delta wing ($\mathcal{R}=2$) in a steady incompressible flow)[a]

Width of region III	C_{L_α}	C_{M_α}	CPU, s
0.30	−2.284	−2.711	5.25
0.20	−2.253	−2.668	5.50
0.10	−2.208	−2.613	5.99
0.06	−2.196	−2.589	5.91
0.02	−2.191	−2.559	5.98

[a] See footnotes 1-5, 7.

The integral in Eq. (1) is evaluated by dividing the wing into four regions (Fig. 3) and performing the numerical integration separately in each of these regions. The most problematic region is III, where the strongest singularity exists. The size of region III is invariably taken to be 30% of the wing semispan (following the recommendations of Ref. 4). This size of region III is clearly unacceptable for the present method since the size of the boxes employed in this method is dictated by the geometrical singularities and, therefore, region III might extend over a number of spanwise boxes (or part of them). This state of affairs is considered to be unfavorable since it involves spanwise integration of discontinuous pressure polynomials (at the spanwise boundaries between the boxes) and therefore is in contradiction with the assumptions of continuity (except for the second-order pole) normally made while performing the spanwise integration in region III. It was therefore decided to investigate the problems associated with the reduction in size of this critical region.

Table 1 shows the effect of varying the spanwise size of region III on the convergence of the aerodynamic coefficients (using Gauss integration in regions II and IV with each wing representing a single box). The poor conditioning of the problem is apparent from the large variations in the values obtained.

At this stage, it is realized that the reduction in size of region III leads to two contradicting effects. The first effect is beneficial since the narrowing of region III permits the representation of the spanwise variation of the integrand by lower order polynomials. The second effect is detrimental since the narrowing of region III brings regions II and IV much closer to the second-order pole situated in region III. Thus, the improvement in the accuracy of integration in region III is accompanied by a severe deterioration in accuracy in regions II and IV. To overcome this problem, it was decided to perform the integrations by allowing for the second-order singularity while performing the integrations in regions II and IV. The method adopted for this purpose was proposed by Demarais[5] and is based essentially on orthogonal polynomial considerations. Table 2 shows the effect of improving the integration procedure in regions II and IV on the results obtained using different spanwise sizes of region III, for the delta wing discussed in Table 1. The results can clearly be seen to be converged and it may be concluded that region III can now be decreased to assume very small spanwise sizes. The default value for the size of region III was chosen to be 0.02 of the wing semispan (instead of the customary size of 0.3).

Table 3 Influence of varying the number of integration points in the chordwise direction (delta wing ($\mathcal{R}=2$) in a steady incompressible flow)[a]

No. of integration points in each of two chordwise subregions	C_{L_α}	C_{M_α}	CPU, s
4	−2.327	−2.823	4.48
6	−2.275	−2.727	5.14
8	−2.251	−2.672	5.72
10	−2.235	−2.636	6.34
12	−1.934	−2.473	7.02
14	-2.688×10^{-5}	-2.862×10^{-5}	7.78

[a] See footnotes 1,4,5,8-10.

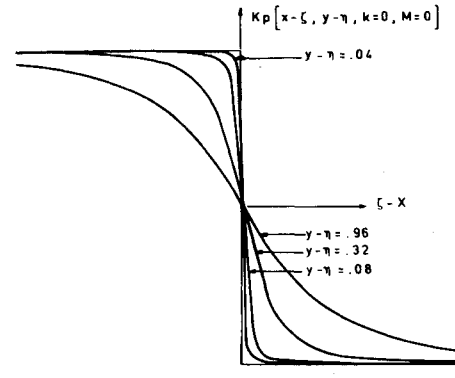

Fig. 4 Chordwise variation of reduced kernel function.

Chordwise Integration of the Kernel-Downwash Expression

The narrowing of region III gave rise to problems associated with the chordwise integration of the kernel-downwash expression in region III. Here again, the results shown in Table 3 indicate poor conditioning of the numerical problem since an increase in the number of chordwise integration points gives rise to numerical instability. This problem was traced to the rapid variations of the kernel in the chordwise direction around the downwash point (that is, around the location of the second-order pole) as shown in Fig. 4. The chordwise integration stages in region III followed initially the commonly used ones. That is, integration was performed in two parts: one part spanned the region between the LE and the downwash point and the second part spanned the region between the downwash point and the TE. By using a small number of integration points in what is now a narrow

‡Footnotes for Tables 1-8:1) The integration in region III is performed by the spanwise expansion of the chordwise integrand into a polynomial of the fourth degree. 2) Four integration points in each of the chordwise subregions. 3) Four spanwise integration points in each of the two wings. 4) The pressure is described by second-degree polynomials in the spanwise and chordwise directions. 5) The moment is about the wing's apex with reference chord = 1 and chord = 2. 6) Integration in regions II and IV is performed using the Gauss method. 7) Integration in regions II and IV is performed by orthogonal polynomials corresponding to the second-order pole singularity. 8) Width of region III is 0.02 of the wing semispan. 9) The chordwise integration is performed as recommended in Ref. 4 (the chord is divided into two subregions: from the LE to the collocation point and from the collocation point to the TE). 10) Six spanwise integration points in each of the two wings. 11) Three integration points in each of the chordwise subregions. 12) Six integration points in each of the chordwise subregions. 13) Four integration points in each of the chordwise subregions.

region III, these points lie essentially on a plateau which describes the behavior of the reduced kernel expression (see Fig. 4). An increase in the number of spanwise integration points will ultimately place an integrating point in the rapidly varying region of the kernel near the collocation point. Since it is clear that a single integration point in a rapidly varying region is unable to define the variation (and it generates a wavy polynomial fit), erroneous and unconverged results might be expected as indicated in Table 3.

To overcome this problem and to account for the chordwise waviness of the unsteady compressible kernel, the chordwise integration in region III was divided into the six subregions indicated in Fig. 5. The boundaries between the various subregions are a function of $|y-\eta|\beta$ as given by the following expressions for values of $|y-\eta|\beta \leq 0.3$:

For chordwise integration subregion 3 and 4

$$0 \leq |\zeta - x| \leq |y-\eta|\beta$$

For chordwise integration subregion 2 and 5

$$|y-\eta|\beta < |\zeta - x| \leq 5\,|y-\eta|\beta$$

For chordwise integration subregion 1 and 6

$$|\zeta - x| > 5\,|y-\eta|\beta$$

where $\beta = \sqrt{1-M^2}$.

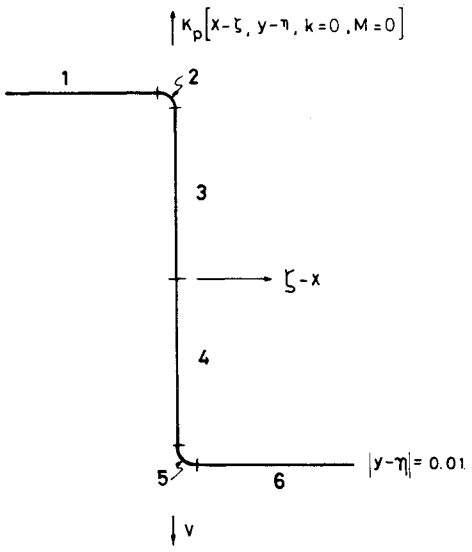

Fig. 5 Division into six subregions to accomplish chordwise integration.

Incorporation of the above integration procedure into the computer program gives rise to a stable and rapidly converging numerical integration system. Table 4 shows the effects of varying the number of integration points in each of the six chordwise integration subregions mentioned above. As can be seen, convergence is rapid and the value of three integration points in each region (see Table 4) was selected as the default value in the computer program developed. For regions over the wing where $|y-\eta|\beta > 0.3$ and also when treating the unsteady part of the compressible kernel (all over the wing), the chordwise integration was performed over subregions in order to account for the waviness of the unsteady compressible kernel function. The size of each of these subregions is determined by the expression $\beta/1.6k$, provided this size is smaller than the local chord.

It might be of interest to mention at this stage that the inclusion of the numerical schemes described above always yields stable and converged results. Under no circumstances is there any need to treat explicitly the logarithmic singularity of the kernel function as suggested in Ref. 6.

Preliminary Results for Single-Box Wings

In the following, preliminary results will be presented with the objective of establishing either the concepts or the numerical values for the different parameters involved in the numerical integration of the kernel-downwash expression. Table 5 shows a comparison between the results obtained using two different sets of spanwise collocation points. The first set is defined by the method outlined earlier in this work, whereas the second set is obtained following the values given by Multhopp.

It is interesting to note that for the case of a rectangular wing, where no geometrical discontinuities occur, the difference between the two sets of results in negligible. On the other hand, for the case of the delta wing where a geometrical discontinuity exists at the wing root, the difference between the two sets of results is significant. The collocation points

Table 4 Influence of varying the number of integration points in each chordwise subregion on the convergence of the aerodynamic coefficients (delta wing ($\mathcal{R}=2$) in a steady incompressible flow)[a]

No. of integration points in each of six chordwise subregions	C_{L_α}	C_{M_α}	CPU, s
2	−2.083	−2.423	6.24
3	−2.185	−2.573	6.79
4	−2.186	−2.574	7.38
6	−2.204	−2.601	8.54
8	−2.205	−2.602	9.69
10	−2.205	−2.601	10.92

[a] See footnotes 1,4,5,8-10.

Table 5 Influence of the location of the spanwise collocation points on the convergence of the aerodynamic coefficients[a]

No. of pressure polynomials		Using PCKFM collocation points			Using Multhopp's collocation points		
Chordwise	Spanwise	C_{L_α}	C_{M_α}	CPU, s	C_{L_α}	C_{M_α}	CPU, s
		Rectangular wing ($\mathcal{R}=1$) in a steady incompressible flow					
3	3	−1.462	−0.491	8.68	−1.469	−0.488	8.23
3	4	−1.461	−0.491	11.00	−1.462	−0.492	10.79
3	5	−1.461	−0.491	14.47	−1.461	−0.491	14.39
		Delta wing ($\mathcal{R}=2$) in a steady incompressible flow					
3	3	−2.204	−2.601	8.13	−2.075	−2.475	7.6
3	4	−2.218	−2.612	10.55	−2.416	−2.749	10.11
3	5	−2.206	−2.604	13.55	−1.911	−2.288	13.27

[a] See footnotes 1,5,8,10,12.

Table 6 Influence on the aerodynamic coefficients of varying the degree of the spanwise polynomial expansion in region III (delta wing ($\mathcal{R}=2$) in steady incompressible flow)[a]

Degree of spanwise polynomial in region III	C_{L_α}	C_{M_α}	CPU, s
0	−2.263	−2.647	4.63
2	−2.198	−2.569	5.22
4	−2.191	−2.559	5.98
6	−2.188	−2.554	7.08
8	−2.185	−2.550	8.24

[a] See footnotes 1, 3-5, 8.

Table 7 Influence of varying the number of spanwise integration points on each wing on the convergence of the aerodynamic coefficients (delta wing ($\mathcal{R}=2$) in a steady incompressible flow)[a]

No. of integration points on each wing	C_{L_α}	C_{M_α}	CPU, s
2	−2.185	−2.521	5.73
3	−2.189	−2.550	5.85
4	−2.191	−2.559	5.98
6	−2.180	−2.574	6.55
8	−2.186	−2.574	7.03
10	−2.184	−2.568	7.59

[a] See footnotes 1,4,5,8,13.

Table 8 Effect of varying the number of the spanwise and chordwise pressure polynomials on the convergence of the aerodynamic coefficients (delta wing ($\mathcal{R}=2$) in a steady incompressible flow)[a]

No. of spanwise pressure polynomials	C_{L_α}	C_{M_α}	CPU, s
Influence of varying number of spanwise pressure polynomials (number of chordwise pressure polynomials = 3)			
2	−2.272	−2.645	5.56
3	−2.204	−2.601	8.02
4	−2.218	−2.612	10.56
6	−2.205	−2.606	16.91
8	−2.204	−2.605	24.95
Influence of varying number of chordwise pressure polynomials (number of spanwise pressure polynomials = 3)			
2	−2.188	−2.628	5.47
3	−2.204	−2.601	8.02
4	−2.220	−2.597	11.61
6	−2.202	−2.591	22.07
8	−2.200	−2.595	37.40

[a] See footnotes 1,5,8,10,12.

developed in this work appear to yield results which are considerably more effective than those obtained while using Multhopp's points.

The effect of varying the degree of the spanwise polynomial series expansion (in region III) on the aerodynamic coefficients is shown in Table 6. An expansion to a 2 degree polynomial was chosen as a default value in the program.

The influence of varying the number of the spanwise integration points is shown in Table 7. Here again, a relatively large number of integration points was chosen (i.e., three in each wing region) as the default value for the computer program developed, although a smaller number of integration points appears to yield satisfactory results.

Finally, the effect of varying the number of orthogonal pressure polynomials on the convergence of the aerodynamic coefficients is shown in Table 8. Here again, the whole wing represents a single box. It can be seen that the convergence obtained is extremely rapid and that two pressure polynomials (that is, linear variation) are sufficient to yield excellent results. Nevertheless, the value of three orthogonal pressure polynomials per box (implying quadratic variation beyond the assumed wing boundary singularities) was chosen as default value for the computer program.

Additional results and comparison between results obtained by applying different methods on single-box wings are presented in a subsequent paper.

Conclusion

An attempt is made in the present work to extend the two-dimensional results of the PCKFM to three-dimensional problems. Consideration is given to the selection of the spanwise orthogonal pressure polynomials and it is shown that best spanwise locations of the collocation points vary considerably from those given by Multhopp. Considerable attention has been focused on numerical integration techniques which need development as a result of the extension of the method to three-dimensional problems. These techniques are valid beyond the method proposed herein and can be incorporated in other methods.

Additional results relating to single-box wings and to wings with multigeometrical singularities along their span (as for example, in wings with break points and control surface deflections) are presented in Parts II and III of this paper.

Appendix: Location of the Collocation Points

The relationship between the pressure distribution and its associated downwash is given by the following well-known expression

$$w(x,y) = \frac{1}{8\pi}\int_S\int \frac{\Delta p(\zeta,\eta)}{q} K[x-\zeta, y-\eta, k, M]\,d\zeta d\eta \quad \text{(A1)}$$

For the problems dealt with in this paper, the downwash distribution is assumed to be known and the pressure distribution that satisfies Eq. (A1) is sought. The kernel function methods are based on the use of n assumed pressure modes which involve the n modal constants as unknowns. These n unknowns are determined by satisfying Eq. (A1) at n different locations along the wing, that is, at n different (x,y) points on the wing. The solution depends therefore on the choice of the pressure modes and collocation points.

For rapid convergence with the number of pressure modes of the resulting pressure forces acting on the lifting surface, the use of orthogonal pressure polynomials is recommended. These orthogonal polynomials take account of the known pressure singularities which exist along the boundaries of the wing (such as the LE, TE, and wing-tip singularities) so as to yield minimum least-square deviations of integrated pressure values such as those associated with the lift and the moment forces. Furthermore, the lift force can be shown to depend on the modal constant associated with the assumed lowest order orthogonal pressure polynomials only. The first moments can similarly be shown to depend on the constants associated with the two lowest order orthogonal pressure polynomials only. This is similar to the well-known results associated with the thin airfoil theory and the lifting line theory. It would however be incorrect to state that only two orthogonal modes need to be assumed in both x and y directions in order to obtain converged integrated forces and moments since the numerical values of the first modal coefficients depend on the number of orthogonal pressure modes used in the analysis. It is therefore of extreme importance to seek a numerical method which will insure the rapid convergence of the low-order modal coefficients so as to take full advantage of the orthogonal polynomial representation of the pressure. The only degrees of freedom available for achieving the rapid convergence of the modal coefficients lie in the choice of the collocation points where Eq. (A1) is satisfied. Reference 3 treats a similar problem using a different approach than the one presented herein. In order to illustrate the underlying principle and to avoid unnecessarily lengthy expressions,

consider the two-dimensional kernel expression which forms the equivalent of Eq. (A1) in two-dimensional flow

$$w(x) = \int_c \frac{\Delta p(\zeta)}{q} K(x-\zeta,k,M)\,d\zeta \qquad \text{(A2)}$$

Let the pressure be represented by a family of n pressure polynomials $p_i(\zeta)$ which are orthogonal to the singularities represented by $W(\zeta)$ and are arranged in increasing order, i.e.

$$\frac{\Delta p(\zeta)}{q} = W(\zeta) \sum_{i=0}^{n-1} A_i p_i(\zeta)$$

where i represent the order of the polynomials. By satisfying Eq. (A2) at n different values of x_j the following n equations are obtained, which lead to the solution for the various A_i.

$$\{w(x_i)\}_{1,n} = [\{D_0\}\{D_1\}\ldots\{D_{n-1}\}]\{A_i\}_{0,(n-1)} \qquad \text{(A3)}$$

where the downwash column is denoted by

$$\{w(x_i)\}_{1,n} = \lfloor w(x_1)\,w(x_2)\ldots w(x_n)\rfloor^T$$

The superfix T denotes the transpose matrix and $\{A_i\}$ denotes the pressure coefficients column, i.e.,

$$\{A_i\}_{0,n-1} = \lfloor A_0, A_1 \ldots A_{n-1}\rfloor^T$$

Each column represented by $\{D_i\}$ is obtained by using the pressure polynomials $p_i(\zeta)$ and collocating at various x_j locations.

Assume that twice as many polynomials are used while collocation is maintained at the same x_j values as in Eq. (A3); the resulting downwash equation will assume the following form

$$\{w(x_i)\}_{1,n} = [\{D_0\}\{D_1\}\ldots\{D_{n-1}\}]\{A_i\}_{0,(n-1)} + [\{D_n\}\ldots\{D_{2n-1}\}]\{A_i\}_{n,(2n-1)} \qquad \text{(A4)}$$

where

$$\{A_i\}_{n,(2n-1)} = \lfloor A_n A_{n+1}\ldots A_{2n-1}\rfloor^T$$

The column $\{A_i\}_{n,(2n-1)}$ can be isolated from Eq. (A4) to yield

$$\{A_i\}_{n,(2n-1)} = [\{D_n\}\ldots\{D_{2n-1}\}]^{-1}(\{w(x_i)\}_{1,n} - [\{D_0\}\ldots\{D_{n-1}\}]\{A_i\}_{0,(n-1)}) \qquad \text{(A5)}$$

If we choose the values of x_j so that they render any of the columns D_i $(i>n-1)$ equal to zero, then the inverted matrix in Eq. (A5) clearly becomes singular leading to the following requirement that emerges from Eq. (A5)

$$\{w(x_i)\}_{1,n} = [\{D_0\}\ldots\{D_{n-1}\}]\{A_i\}_{0,n-1} \qquad \text{(A6)}$$

The result indicated by Eq. (A6) is very interesting since it enables direct determination of the column of unknowns $\lfloor A_0 \ldots A_{n-1}\rfloor^T$ without resorting to the solution for the higher A_i coefficients. In other words, the accuracy obtained for the first n modal coefficients A_i is equivalent to the one obtained while using $2n$ modal coefficients.

The solution of Eq. (A6) is given by

$$\{A_i\}_{0,(n-1)} = [\{D_0\}\ldots\{D_{n-1}\}]^{-1}\{w(x_i)\}_{1,n} \qquad \text{(A7)}$$

where the x_j values nullify any $\{D_i\}$ with $i>n-1$.

Experience shows that by increasing i by 1 [that is increasing the order of the orthogonal pressure polynomial to $(i+1)$], the number of zeros of $\{D_i\}$ are increased by one. In other words, the number of zeros of $\{D_i\}$ increase linearly with i. Hence $\{D_n\}$ will have at least n zeros in the chordwise range of x. The column $\{D_{2n-1}\}$ will have $(n-1)$ additional zeros compared to $\{D_n\}$. For best conditioning of the matrix inverted in Eq. (A7), it is recommended to use the zeros of $\{D_n\}$. These zeros can be readily determined numerically by collocating at a large number of points using $P_n(\zeta)$.

For the general finite-wing case, the argumentation presented above is identical with one exception: It is possible to nullify more than a single column of $\{D_i\}$ [with $i>(n-1)$]. For highest order degeneracy of the matrix needing inversion [see Eq. (A5)] and for best conditioning of the low-order coefficients matrix [see Eq. (A7)], it is recommended in the x direction to use the zeros defined by $\{D_r\}$. These zeros are associated with the orthogonal polynomial of order r in the x direction and of order zero in the y direction. Similarly, in the y direction, it is recommended to use the zeros defined by $\{D_p\}$. These zeros are associated with the orthogonal polynomial of order zero in the x direction and of order p in the y direction. In this case the total number of unknown pressure modal coefficients is given by

$$n = rp$$

and the downwash zeros are equal to or greater than n. For the case when the number of downwash zeros exceeds the number of unknowns, solution is obtained by least-square methods.

For the sake of completeness, we mention here the location of the collocation points that were taken in the chordwise direction for the three main boxes (box with LE singularity, box with TE singularity, and the intermediate boxes without prescribed singularity):

LE box $\quad (W(\zeta) = 1/\sqrt{1+\zeta})$

$$x_c = \cos\frac{4j\pi}{4M_1+1} \qquad j=1,2,\ldots,M_1$$

TE box $\quad (W(\zeta) = \sqrt{1-\zeta})$

$$x_c = \cos\frac{(4j-3)\pi}{4M_n-1} \qquad j=1,2,\ldots,M_n$$

Intermediate box $\quad (W(\zeta) = 1)$

$$x_c = \cos\frac{(3j-2)\pi}{3M_1-1} \qquad j=1,2,\ldots,M_1$$

Acknowledgment

This work represents a part of the first author's doctoral thesis.

References

[1] Nissim, E. and Lottati, I., "Oscillatory Subsonic Piecewise Continuous Kernel Function Method," National Technical Information Service, Springfield, Va., Paper N77-73109, 1977.

[2] Nissim, E. and Lottati, I., "Oscillatory Subsonic Piecewise Continuous Kernel Function Method," *Journal of Aircraft*, Vol. 14, June 1977, pp. 515-516.

[3] Hsu, P.T., "Some Recent Developments in the Flutter Analysis of Low-Aspect-Ratio Wings," *Proceedings of National Specialists Meeting on Dynamics and Aeroelasticity*, Institute of Aeronautical Sciences, Nov. 1958, pp. 7-26.

[4] Watkins, C.E., Woolston, D.S., and Cunningham, H.J., "A Systematic Kernel Function Procedure for Determining Aerodynamic Forces on Oscillating or Steady Finite Wings at Subsonic Speeds," NASA TR-48, 1959.

[5] Desmarais, R.N., "Programs for Computing Abscissas and Weights for Classical and Non-Classical Gaussian Quadrature Formulas," NASA TN-D-7924, Oct. 1975.

[6] Zandbergen, P.J., Labrujere, Th.E., and Wouters, J.G., "A New Approach to the Numerical Solution of the Equation of Subsonic Lifting Surface Theory," NLR TR G. 49, Nov. 1979.